

Space Environmental Performance of Optical Coatings on Tedlar

15 November 2000

Prepared by

W. K. STUCKEY, J. D. BARRIE, and M. J. MESHISHNEK
Space Materials Laboratory
Laboratory Operations

Prepared for

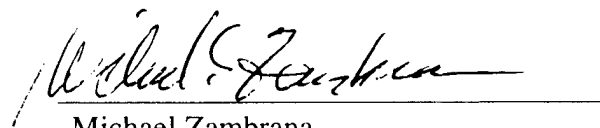
SPACE AND MISSILE SYSTEMS CENTER
AIR FORCE MATERIEL COMMAND
2430 E. El Segundo Boulevard
Los Angeles Air Force Base, CA 90245

Engineering and Technology Group

This report was submitted by The Aerospace Corporation, El Segundo, CA 90245-4691, under Contract No. F04701-93-C-0094 with the Space and Missile Systems Center, 2430 E. El Segundo Blvd., Los Angeles Air Force Base, CA 90245. It was reviewed and approved for The Aerospace Corporation by P. D. Fleischauer, Principal Director, Space Materials Laboratory. Michael Zambrana was the project officer for the Mission-Oriented Investigation and Experimentation (MOIE) program.

This report has been reviewed by the Public Affairs Office (PAS) and is releasable to the National Technical Information Service (NTIS). At NTIS, it will be available to the general public, including foreign nationals.

This technical report has been reviewed and is approved for publication. Publication of this report does not constitute Air Force approval of the report's findings or conclusions. It is published only for the exchange and stimulation of ideas.

A handwritten signature in black ink, appearing to read "Michael Zambrana", is written over a horizontal line.

Michael Zambrana
SMC/AXE

REPORT DOCUMENTATION PAGE			Form Approved OMB No. 0704-0188	
Public reporting burden for this collection of information is estimated to average 1 hour per response, including the time for reviewing instructions, searching existing data sources, gathering and maintaining the data needed, and completing and reviewing the collection of information. Send comments regarding this burden estimate or any other aspect of this collection of information, including suggestions for reducing this burden to Washington Headquarters Services, Directorate for Information Operations and Reports, 1215 Jefferson Davis Highway, Suite 1204, Arlington, VA 22202-4302, and to the Office of Management and Budget, Paperwork Reduction Project (0704-0188), Washington, DC 20503.				
1. AGENCY USE ONLY (Leave blank)		2. REPORT DATE 15 November 2000		3. REPORT TYPE AND DATES COVERED
4. TITLE AND SUBTITLE Space Environmental Performance of Optical Coatings on Tedlar			5. FUNDING NUMBERS F04701-00-C-0009	
6. AUTHOR(S) W. K. Stuckey, J. D. Barrie, and M. J. Meshishnek				
7. PERFORMING ORGANIZATION NAME(S) AND ADDRESS(ES) The Aerospace Corporation Laboratory Operations El Segundo, CA 90245-4691			8. PERFORMING ORGANIZATION REPORT NUMBER TR-2001(8565)-1	
9. SPONSORING/MONITORING AGENCY NAME(S) AND ADDRESS(ES) Space and Missile Systems Center Air Force Materiel Command 2430 E. El Segundo Boulevard Los Angeles Air Force Base, CA 90245			10. SPONSORING/MONITORING AGENCY REPORT NUMBER SMC-TR-01-02	
11. SUPPLEMENTARY NOTES				
12a. DISTRIBUTION/AVAILABILITY STATEMENT Approved for public release; distribution unlimited			12b. DISTRIBUTION CODE	
13. ABSTRACT (Maximum 200 words) <p>A space environment exposure test has been performed on a variety of samples of Cloud White Tedlar with a multi-layer thin-film coating on the surface applied by Optical Coatings Laboratory, Inc. (OCLI) representing potential spacecraft applications. This test was performed to evaluate new coating formulations.</p> <p>The Tedlar coated with the new formulations was compared with previously coated Tedlar material. For the coated Tedlar on foam samples, the Ta₂O₅/ZrO₂ configuration appeared to perform best and was comparable to the original coating configuration. Tedlar film samples were in general agreement with the foam samples, although all film samples with the new coatings appeared to degrade more than the films with the original coating. Changes in coatings on fused silica were very small. Degradation of the coated Tedlar is apparently due to changes in the Tedlar substrate, not the coating. The advantages in the newer coating configuration could well be in easier fabrication and improved adhesion.</p>				
14. SUBJECT TERMS Space simulation, Space radiation, Space environmental effects, Spacecraft materials, Thermal control materials			15. NUMBER OF PAGES 13	
			16. PRICE CODE	
17. SECURITY CLASSIFICATION OF REPORT UNCLASSIFIED	18. SECURITY CLASSIFICATION OF THIS PAGE UNCLASSIFIED	19. SECURITY CLASSIFICATION OF ABSTRACT UNCLASSIFIED	20. LIMITATION OF ABSTRACT	

Contents

1. Introduction	1
2. Experimental.....	3
3. Results.....	7
4. Conclusions	13

Figures

1. The Space Environmental Effects Chamber.	3
2 Sample arrangement in the Space Environmental Effects Chamber.....	5
3. Plot of solar absorptance changes of control samples.....	7
4. Change in solar absorptances with exposure time to solar radiation.....	8
6. Bar graph display of solar absorptance data for radome samples.	10
7. Plot of the change in transmission vs wavelength for the six OCLI-coated fused-silica disks listed in Table 3.....	11
8. Plot of sample transmission before and after UV exposure for two OCLI-coated fused-silica samples.....	11

Tables

1. List of Samples.....	4
2. Pre-test and Post-test Solar Absorptance of Radome and Control Samples	9
3. Pre-test and Post-test Solar Absorptance and Transmittance of Thin Samples	9

1. Introduction

Tedlar is a polyvinyl fluoride film produced by E. I. DuPont de Nemours & Co. (Inc.) with a variety of additives that can be introduced to produce different properties. The designations code of TWH is for a white Tedlar film and a TCW designation is indicative for a Cloud White version that has a lower solar absorptance (is a whiter material). The full designation for these products, for example, TCW20BE3, identifies color, thickness, surface finish, gloss, and type of elongation properties. Cloud White Tedlar with a multi-layer thin-film coating on the surface applied by Optical Coatings Laboratory, Inc. (OCLI) is being investigated for a number of potential spacecraft applications. Space environment exposure tests have been performed previously on a variety of samples exposed to simulated Low Earth Orbit (LEO) conditions.

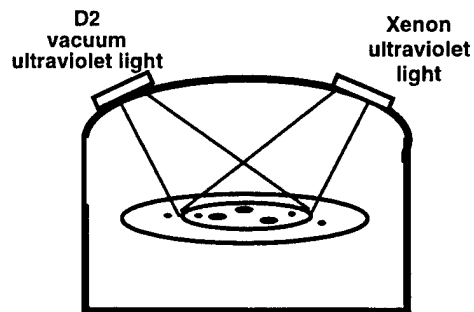
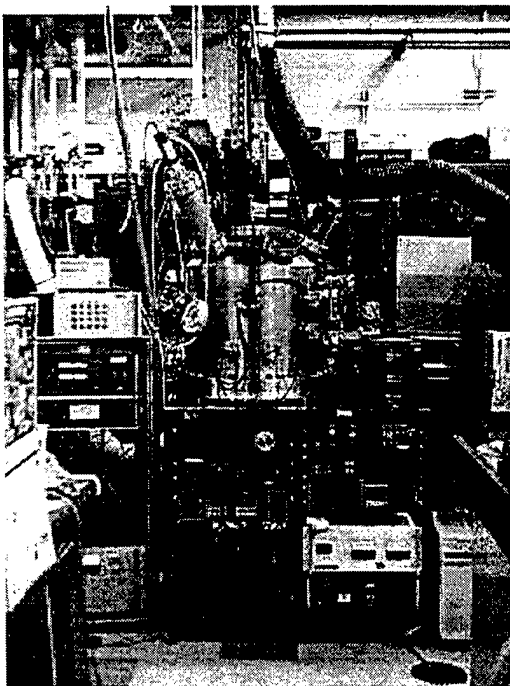
This test was performed to evaluate various coating formulations that can be applied to Tedlar. The ideal coating would provide blockage of the damaging part of the solar ultraviolet (UV) spectrum in the vacuum UV range and be well adhered so that subsequent testing, handling, and temperature and humidity exposures under reasonable conditions would not degrade the performance of the coating.

Three variations of optical coatings were included in this test. The older process used for previous evaluations in this laboratory is identified by the 1029 designation. A newer approach by OCLI is identified by the 1047 designation. This approach changes the deposition process with accompanying changes in the adhesion approach and layer composition but offers the advantage of a more controlled deposition process. This test was conducted for comparison of the Tedlar coated with the new process and the previously coated Tedlar material.

2. Experimental

The Space Environmental Effects Chamber (Figure 1) used to provide the simulation of the LEO space environment contains a 2500-W xenon arc lamp for long-wavelength UV (230–400 nm) and a 150-W deuterium arc lamp for vacuum ultraviolet (VUV) radiation (115–200 nm). The beams are confocal and have a uniformity within 50% but contain small central hot spots. The chamber is turbopumped, and the base pressure is currently 2×10^{-9} torr. The volume is roughly 200 liters with a sample table 12 in. in diameter capable of temperature control from -150°C to $+150^{\circ}\text{C}$, but kept at about 25°C for these tests. Computerized data acquisition is used for chamber diagnostics, which include several temperature and solar cell measurements. Electrons were not used in this test.

The list of samples is shown in Table 1. The radome-type samples consisted of the Tedlar film, with various coatings or without a coating, bonded with an acrylic adhesive to a Rohacell foam that could be used for certain radome applications. All of the radome-type samples were about 1 in. square. Samples of optical coatings on 1-in.-dia fused-silica discs were also included. The arrangement of the samples in the chamber for this test is shown in Figure 2. The larger area represents the approximately 12-in.-dia area covered by the xenon lamp. The area covered by the deuterium lamp is about 7 in. in diameter so it does not illuminate all samples in the LEO exposure. The solar cell is used as a diagnostic during the exposure to monitor the xenon lamp output. An Optical Solar Reflector (OSR)



side
view

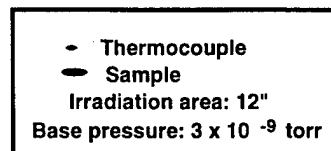


Figure 1. The Space Environmental Effects Chamber.

is present as a check for any contamination if it should condense during the test and might potentially affect test results. There are some samples in Figure 2 that are not in Table 1. Those samples are the subject of a separate report.

The Solar UV exposure was started when the chamber pressure was in the low to mid 10^{-8} torr region. The electrons were not included in this test to compare samples with slightly different histories. During the Solar UV exposure, some samples were removed, and the solar absorptance was measured. Some samples were removed, measured, and replaced at 390, 790, 1260, and 1700 equivalent sun-hours. After 3594 equivalent UV sun hours (1288 h, at a solar intensity of 2.8 suns), the exposure was completed, and all samples were removed and measured. Throughout the entire exposure, the deuterium lamp was cycled on periodically (effectively 4.0 h/day) to accumulate approximately the same number of equivalent UV sun hours as the xenon source. The deuterium source has been estimated to have an initial output of about 17 solar constants over its operating

Table 1. List of Samples

Sample	Description	Comments	Time Measurements
RDM-2083-1	1047-2083 Radome Sample (New OCLI)	ZrO ₂ /SiO ₂ /Si/Tedlar/foam	X
RDM-2083-2	1047-2083 Radome Sample (New OCLI)	ZrO ₂ /SiO ₂ /Si/Tedlar/foam	
RDM-2083-3	1047-2083 Radome Sample (New OCLI)	ZrO ₂ /SiO ₂ /Si/Tedlar/foam	
RDM-2084-1	1047-2084 Radome Sample (New OCLI)	Ta ₂ O ₅ /ZrO ₂ /SiO ₂ /Si/Tedlar/foam	X
RDM-2084-2	1047-2084 Radome Sample (New OCLI)	Ta ₂ O ₅ /ZrO ₂ /SiO ₂ /Si/Tedlar/foam	
RDM-2084-3	1047-2084 Radome Sample (New OCLI)	Ta ₂ O ₅ /ZrO ₂ /SiO ₂ /Si/Tedlar/foam	
RDM-2085-1	1047-2085 Radome Sample (New OCLI)	ZrO ₂ /SiO ₂ (2 stacks)/Si/Tedlar/foam	X
RDM-2085-2	1047-2085 Radome Sample (New OCLI)	ZrO ₂ /SiO ₂ (2 stacks)/Si/Tedlar/foam	
RDM-2085-3	1047-2085 Radome Sample (New OCLI)	ZrO ₂ /SiO ₂ (2 stacks)/Si/Tedlar/foam	
TD-2083	1047-2083 Tedlar Film (New OCLI)	ZrO ₂ /SiO ₂ /Si/Tedlar	
TD-2084	1047-2084 Tedlar Film (New OCLI)	Ta ₂ O ₅ /ZrO ₂ /SiO ₂ /Si/Tedlar	
TD-2085	1047-2085 Tedlar Film (New OCLI)	ZrO ₂ /SiO ₂ (2 stacks)/Si/Tedlar	
TD-1029	1029 Film (Old OCLI)	TiO ₂ /SiO ₂ /Ti/Tedlar	
OCLI-1	Coating on Fused Silica Disc	ZrO ₂ /SiO ₂ /Si/ Fused Silica	
OCLI-2	Coating on Fused Silica Disc	Ta ₂ O ₅ /ZrO ₂ /SiO ₂ /Si/ Fused Silica	
OCLI-3	Coating on Fused Silica Disc	ZrO ₂ /SiO ₂ (2 stacks)/Si/ Fused Silica	
OCLI-4	Coating on Fused Silica Disc	TiO ₂ /SiO ₂ /Ti/ Fused Silica	
OCLI-5	Coating on Fused Silica Disc	TiO ₂ /SiO ₂ /Ti/ Fused Silica	
OCLI-6	Coating on Fused Silica Disc	ZrO ₂ /SiO ₂ /Si/ Fused Silica	
OSR	Optical Solar Reflector	Contamination Monitor	X
A-276	A-276 Paint Sample	Control Sample	X
Solar Cell	Solar Cell	Solar Radiation Monitor	

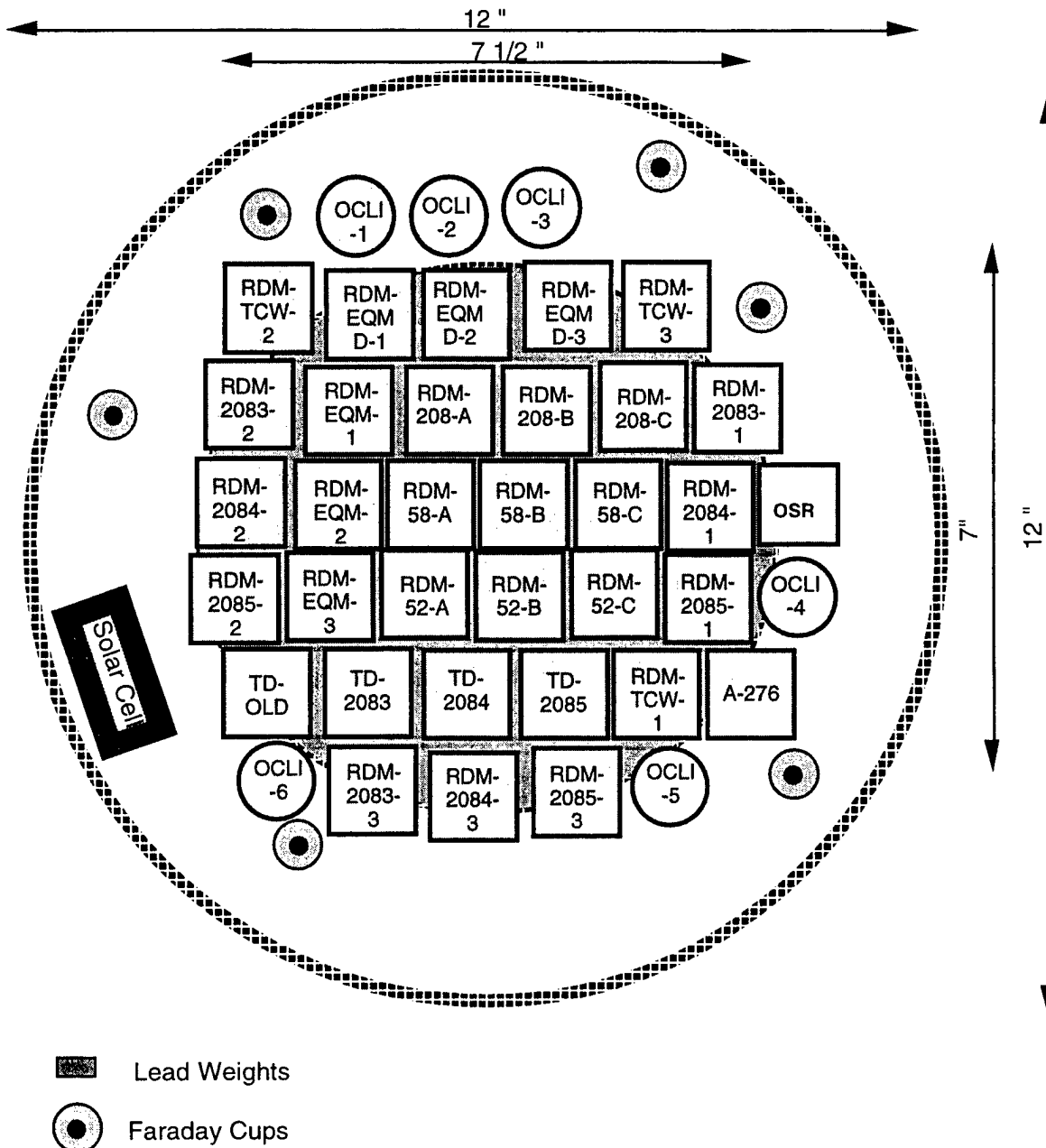


Figure 2 Sample arrangement in the Space Environmental Effects Chamber.

wavelength range, as compared to about 2.8 for the xenon source. The xenon source output is spectrally calibrated pretest using a calibrated spectral radiometer. Relative intensity over the sample area is mapped with a solar cell.

The following method was used to obtain the solar reflectance, transmittance, and absorptance. The Ultraviolet-Visible-Near Infrared (UV-VIS-NIR) diffuse hemispherical reflectance was measured on a Perkin-Elmer Lambda-9 equipped with a 6-in. Labsphere, Inc. Spectralon coated integrating sphere.

The reflectance measurements were made using a 240 nm/min scan rate, 2 nm slit width, and 0.5 s response, with the scan range being 250–2500 nm. The reflectance spectrum was background corrected and referenced to a NIST 2019d White Tile Diffuse Reflectance Standard. This procedure references the sample spectrum to a NIST perfect diffuser rather than the Spectralon integrating sphere coating. Correction factors are calculated and applied to the sample spectrum from the measured NIST Standard. The accuracy of the reflectance measurements is $\pm 2\%$. A trapezoidal approximation to the two integrals that define the ASTM Solar Air Mass Zero curve and the measured reflectance spectrum is then calculated. The calculation involves 137 points corresponding to the 137 wavelength bins that define the ASTM Solar Air Mass Zero curve from 250 to 2500 nm. The calculation of the solar absorptance makes use of the Kirchoff relationship, which states that any energy (or in this case light) that is not reflected or transmitted, must be absorbed. Therefore, the solar absorptance (α) can be calculated from the hemispherical reflectance (ρ) and diffuse transmittance (τ) by the equation: $\alpha = 1 - \rho - \tau$. If the material is opaque, then the transmittance, τ , is zero, and therefore: $\alpha = 1 - \rho$. For transmissive materials (all nonmetallized), the diffuse transmittance was also measured using the same instrumentation; however, there is no correction applied to the sample spectrum beyond the background correction of the machine.

3. Results

Several samples were in the test as exposure controls. Samples of optical solar reflectors (OSRs) were included in the test to monitor for any contamination that might contribute to changes in solar absorptance. The OSRs remained essentially stable so contamination was not a problem. Chemglaze A-276 is a white polyurethane paint with extensive on-orbit data and is typically used in this facility as an exposure control sample. The results from this test for the solar absorptance as a function of exposure time in the chamber are shown in Figure 3. The data from a similar test in 1997 are shown for comparison. The agreement between this test and the 1997 test is very good for A-276. A sample of a radome with uncoated Tedlar material used in the 1997 test was also included as a control sample. Those results do not compare well with the 1997 results. However, it was clearly apparent that the sample in the current test did not darken uniformly as expected. It has a "bleached" appearance that is not what has been typically seen for unprotected Tedlar. The reason for this is not known but it is assumed that some contamination from storage or other effect is responsible. The performance of the A-276 Chemglaze paint, as anticipated, is adequate to confirm that the exposure conditions were satisfactory. The TCW20BE3 Radome sample also indicates the degradation that is typical of uncoated Tedlar.

A set of samples was selected to monitor as a function of exposure time. The data from these samples are plotted in Figure 4 with data from an earlier test for comparison. The low Alpha Radome has the 1029 process material, while the TCW20BE3 Radome indicates the degradation that occurs without

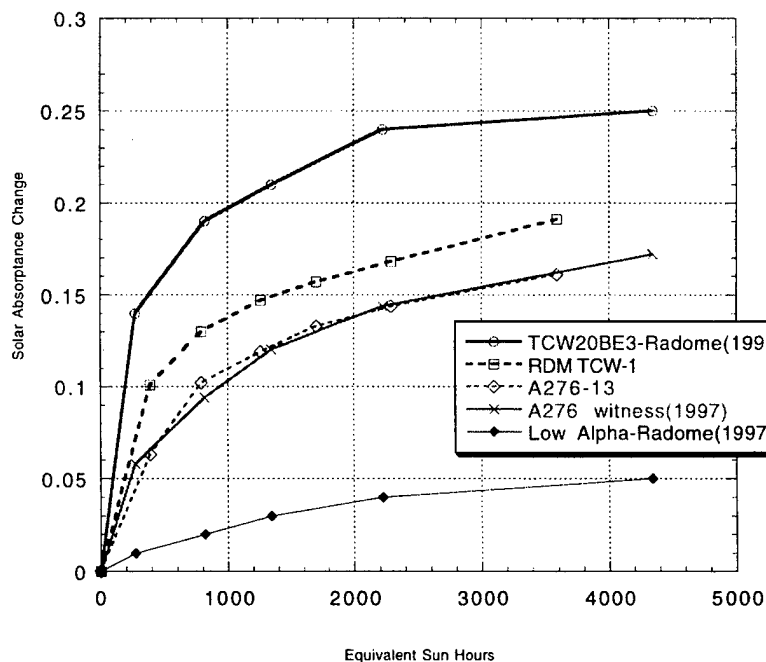


Figure 3. Plot of solar absorptance changes of control samples.

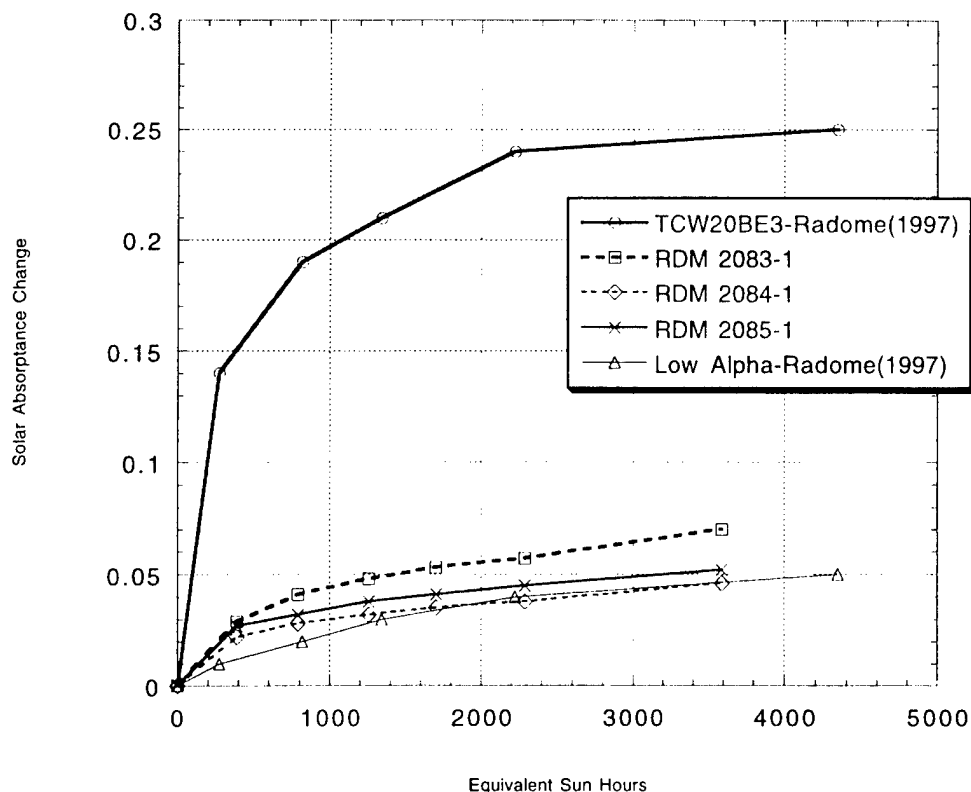


Figure 4. Change in solar absorptances with exposure time to solar radiation.

any coating on the Tedlar. In this data, the RDM 2083-1 with the $\text{ZrO}_2/\text{SiO}_2$ stack shows the higher degradation. The double thickness of this stack, RDM 2085-1, is better. The degradation of the RDM 2084-1 sample, with a stack similar to RDM 2083-1 but with some outer layers of ZrO_2 replaced by Ta_2O_5 , has the lowest degradation and is very similar to the original version of the Low Alpha coating.

The data for solar absorptance for all the radome-type samples are shown in Table 2 and Figure 5. The data measured at the end of the test for all samples shows the same trends indicated in the three samples selected for time measurements. The coating stack of $\text{ZrO}_2/\text{SiO}_2$ with some outer layers of the ZrO_2 replaced with Ta_2O_5 gives the smallest change in solar absorptance for this LEO five-year exposure, similar to that of the original $\text{TiO}_2/\text{SiO}_2$ coating stack.

Samples of the 0.002-in. Tedlar films with the coatings as produced but not mounted onto Rohacell foam substrates were also included. Witness samples from the coating runs on fused-silica discs were also included. Data from those samples are shown in Table 3. For the Tedlar samples, there is some transmittance of the samples so both transmittance and reflectance were measured. The absorptance is calculated as discussed earlier. An apparent small decrease in transmittance is noted in all Tedlar film samples. The same ranking of performance of the coatings is observed in these samples, but the original coating formulation appears to be significantly better than the $\text{Ta}_2\text{O}_5/\text{ZrO}_2/\text{SiO}_2$ for the Tedlar film samples. Smaller differences were observed for the optical coatings on fused silica (Figures 6 and 7). In these samples, the initial transmittance in visible wavelengths is high. After the UV expo-

Table 2. Pre-test and Post-test Solar Absorptance of Radome and Control Samples

Sample #	Identity	Pretest Alpha	Post-test Alpha	Delta Alpha
RDM 2083-1	TD 1047-2083/Tedlar/Radome	0.192	0.262	0.070
RDM 2083-2	TD 1047-2083/ Tedlar/Radome	0.193	0.27	0.077
RDM 2083-3	TD 1047-2083/ Tedlar/Radome	0.193	0.253	0.060
RDM 2084-1	TD 1047-2084/ Tedlar/Radome	0.199	0.245	0.046
RDM 2084-2	TD 1047-2084/ Tedlar/Radome	0.194	0.249	0.055
RDM 2084-3	TD 1047-2084/ Tedlar/Radome	0.198	0.241	0.043
RDM 2085-1	TD 1047-2085/ Tedlar/Radome	0.189	0.241	0.052
RDM 2085-2	TD 1047-2085/ Tedlar/Radome	0.193	0.255	0.062
RDM 2085-3	TD 1047-2085/ Tedlar/Radome	0.193	0.249	0.056
RDM 208 C	208 Radome	0.188	0.238	0.050
RDM EQM C	EQM Radome	0.203	0.247	0.044
RDM TCW-1	Uncoated Tedlar/Radome	0.241	0.432	0.191
RDM TCW-2	Uncoated Tedlar/Radome	0.236	0.404	0.168
RDM TCW-3	Uncoated Tedlar/Radome	0.239	0.457	0.218
A276-13	Chemglaze A-276	0.257	0.418	0.161
SI-100-7	OCLI OSR	0.078	0.080	0.002
SI-100-8	OCLI OSR	0.071	0.086	0.015
SI-100-9	OCLI OSR	0.084	0.081	-0.003
SI-100-13	OCLI OSR	0.091	0.084	-0.007

Table 3. Pre-test and Post-test Solar Absorptance and Transmittance of Thin Samples

Sample #	Identity	Pretest Transmittance	Pretest Alpha	Post-test Transmittance	Posttest Alpha	Delta Alpha
TD 2083-2	ZrO2/SiO2/Si/Tedlar	0.161	0.090	0.157	0.163	0.073
TD 2084-3	Ta2O5/ZrO2/SiO2/Si/Tedlar	0.166	0.088	0.163	0.136	0.048
TD 2085-1	ZrO2/SiO2(2 stacks)/Si/Tedlar	0.161	0.090	0.157	0.150	0.060
TD-1029-1	TiO2/SiO2/Ti/Tedlar	0.163	0.090	0.161	0.123	0.033
TD 1029-2	TiO2/SiO2/Ti/Tedlar	0.162	0.090	0.160	0.125	0.035
		Pretest Transmittance*	Post-test Transmittance	Delta Transmittance		
OCLI-1	ZrO2/SiO2/Si/ Fused Silica	0.826	0.822	-0.004		
OCLI-2	Ta2O5/ZrO2/SiO2/Si/ Fused Silica	0.837	0.832	-0.005		
OCLI-3	ZrO2/SiO2(2 stacks)/Si/ Fused Silica	0.803	0.797	-0.006		
OCLI-4	TiO2/SiO2/Ti/ Fused Silica	0.743	0.749	+0.006**		
OCLI-5	TiO2/SiO2/Ti/ Fused Silica	0.745	0.742	-0.003		
OCLI-6	ZrO2/SiO2/Si/ Fused Silica	0.939	0.931	-0.008		

* Transmittance measured from 400–800 nm. ** Delta for OCLI-4 affected by shift in spectrum, probably due to tilt.

Pre- and Post-Test Solar Absorptance with Alternate Coatings

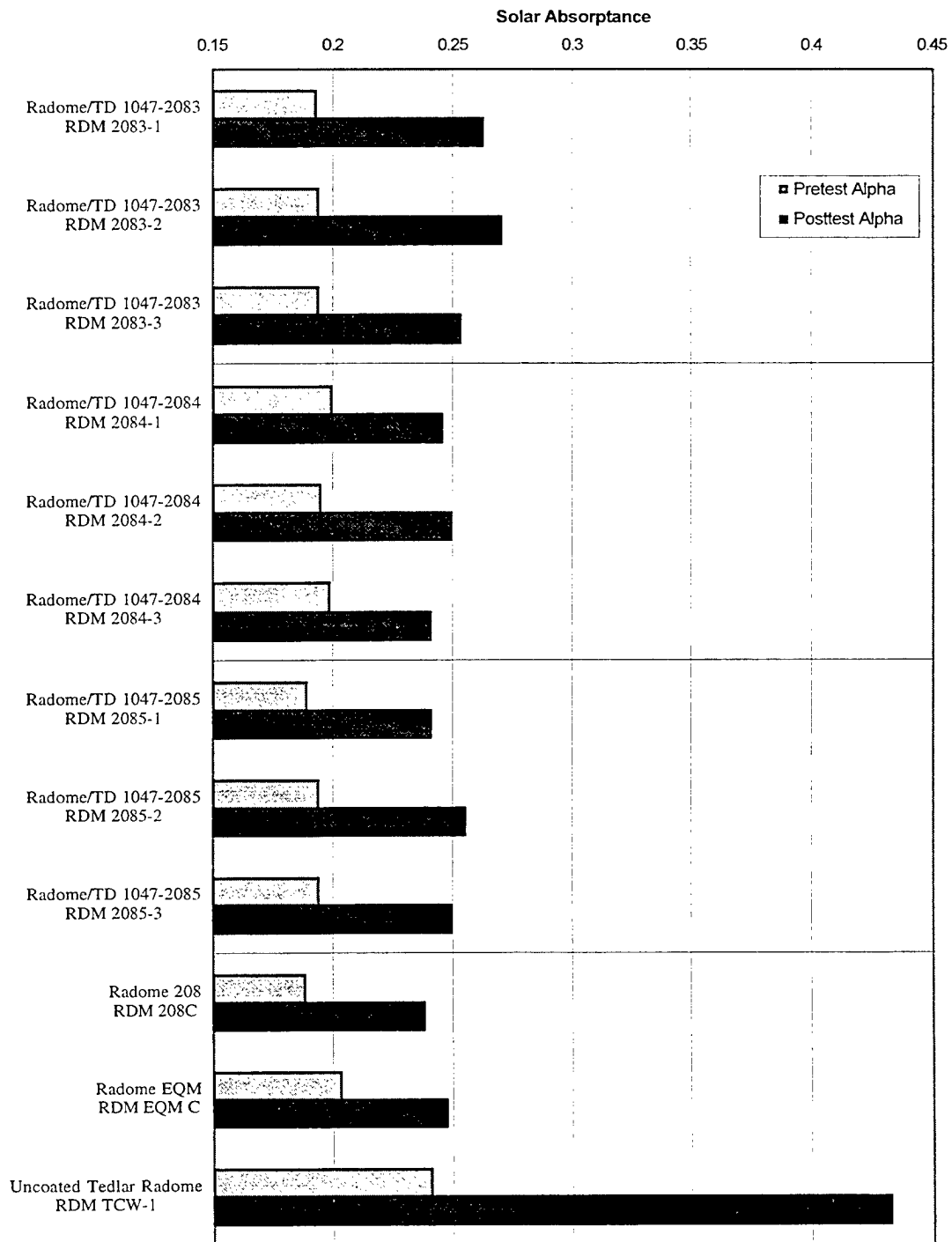


Figure 5. Bar graph display of solar absorptance data for radome samples.

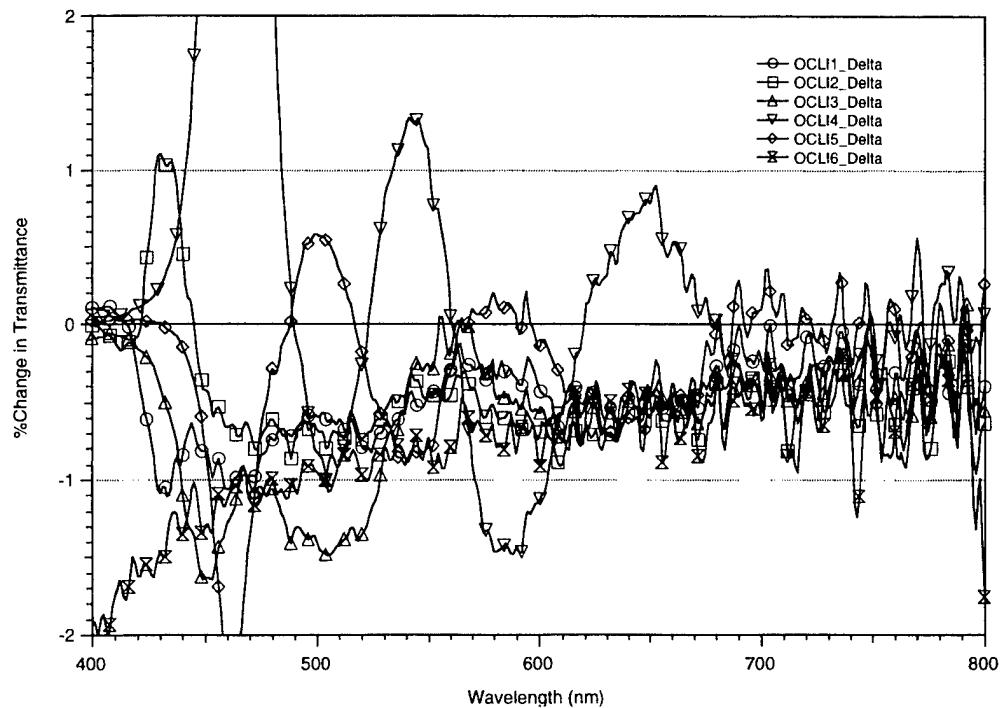


Figure 6. Plot of the change in transmission vs wavelength for the six OCLI-coated fused-silica disks listed in Table 3.

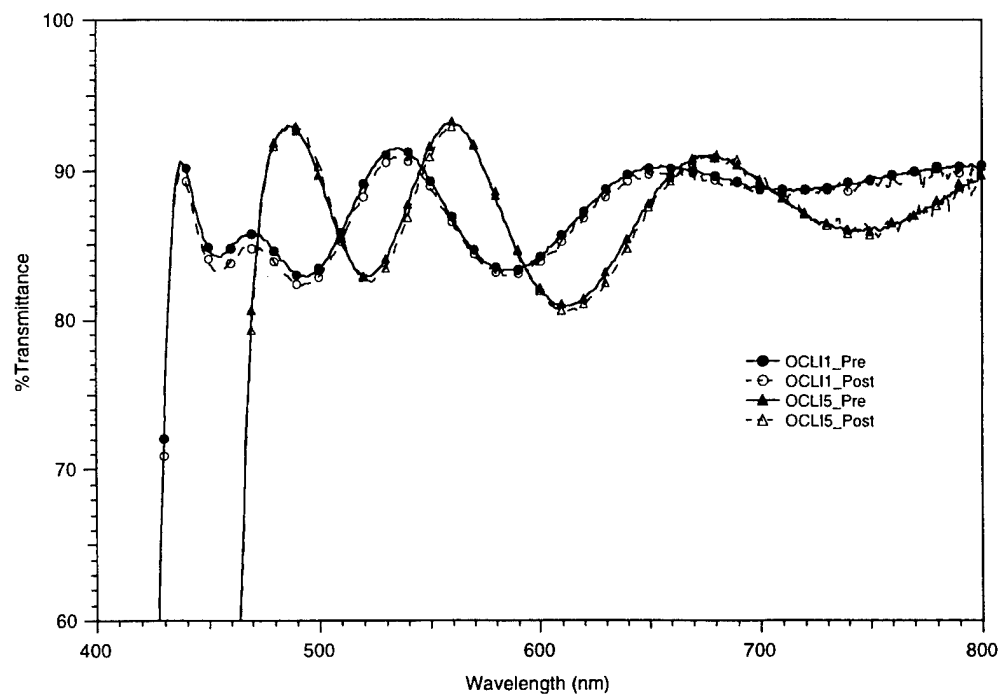


Figure 7. Plot of sample transmission before and after UV exposure for two OCLI-coated fused-silica samples: (1) New $\text{ZrO}_2/\text{SiO}_2$ configuration, (5) Old $\text{Ta}_2\text{O}_5/\text{TiO}_2/\text{SiO}_2$ configuration.

sure, the transmittance of five of the six samples was reduced. One of the samples exhibits an apparent increase in transmittance, which is caused by a shifting of the interference peaks in the sample arising either from a slight tilting of the sample during the posttest measurement or by a densification or outgassing of the sample during the test. While the magnitude of the changes observed is small (less than 1% in transmittance), the trend appears to be real. Furthermore, the changes observed appear to be slightly greater in the recently coated ZrO_2 -containing stacks than in the original configuration coatings based upon TiO_2 . All of these changes are much smaller than observed in the coated Tedlar samples. This could be due to the differences in substrate properties or to the sample position in the chamber that resulted in the lack of VUV on the fused-silica samples.

4. Conclusions

All coatings performed well. For the coated Tedlar on foam samples, the $\text{Ta}_2\text{O}_5/\text{ZrO}_2$ configuration appeared to perform best and was comparable to the original coating configuration. The film samples were in general agreement with the foam samples except that all film samples with the new coatings appeared to degrade more than the films with the original coating. Changes in the coatings on fused silica were very small. Degradation of the coated Tedlar is apparently due to changes in the Tedlar substrate, not the coating. The advantages in the newer coating configuration could well be in easier fabrication and improved adhesion. Adhesion and environmental testing of the new coatings has not been performed.

LABORATORY OPERATIONS

The Aerospace Corporation functions as an "architect-engineer" for national security programs, specializing in advanced military space systems. The Corporation's Laboratory Operations supports the effective and timely development and operation of national security systems through scientific research and the application of advanced technology. Vital to the success of the Corporation is the technical staff's wide-ranging expertise and its ability to stay abreast of new technological developments and program support issues associated with rapidly evolving space systems. Contributing capabilities are provided by these individual organizations:

Electronics and Photonics Laboratory: Microelectronics, VLSI reliability, failure analysis, solid-state device physics, compound semiconductors, radiation effects, infrared and CCD detector devices, data storage and display technologies; lasers and electro-optics, solid state laser design, micro-optics, optical communications, and fiber optic sensors; atomic frequency standards, applied laser spectroscopy, laser chemistry, atmospheric propagation and beam control, LIDAR/LADAR remote sensing; solar cell and array testing and evaluation, battery electrochemistry, battery testing and evaluation.

Space Materials Laboratory: Evaluation and characterizations of new materials and processing techniques: metals, alloys, ceramics, polymers, thin films, and composites; development of advanced deposition processes; nondestructive evaluation, component failure analysis and reliability; structural mechanics, fracture mechanics, and stress corrosion; analysis and evaluation of materials at cryogenic and elevated temperatures; launch vehicle fluid mechanics, heat transfer and flight dynamics; aerothermodynamics; chemical and electric propulsion; environmental chemistry; combustion processes; space environment effects on materials, hardening and vulnerability assessment; contamination, thermal and structural control; lubrication and surface phenomena.

Space Science Application Laboratory: Magnetospheric, auroral and cosmic ray physics, wave-particle interactions, magnetospheric plasma waves; atmospheric and ionospheric physics, density and composition of the upper atmosphere, remote sensing using atmospheric radiation; solar physics, infrared astronomy, infrared signature analysis; infrared surveillance, imaging, remote sensing, and hyperspectral imaging; effects of solar activity, magnetic storms and nuclear explosions on the Earth's atmosphere, ionosphere and magnetosphere; effects of electromagnetic and particulate radiations on space systems; space instrumentation, design fabrication and test; environmental chemistry, trace detection; atmospheric chemical reactions, atmospheric optics, light scattering, state-specific chemical reactions and radiative signatures of missile plumes.

Center for Microtechnology: Microelectromechanical systems (MEMS) for space applications; assessment of microtechnology space applications; laser micromachining; laser-surface physical and chemical interactions; micropropulsion; micro- and nanosatellite mission analysis; intelligent microinstruments for monitoring space and launch system environments.

Office of Spectral Applications: Multispectral and hyperspectral sensor development; data analysis and algorithm development; applications of multispectral and hyperspectral imagery to defense, civil space, commercial, and environmental missions.